공학석사학위논문

광학고온계측법을 이용한 미분 우드펠릿 화염의 온도 측정

Measurement of Pulverized Wood Pellet Flame Temperature using Optical Pyrometry in Lab-scale Burner

2014 년 2 월

서울대학교 대학원

기계항공공학부

송 정 우

광학고온계측법을 이용한 미분 우드펠릿 화염의 온도 측정

Measurement of Pulverized Wood Pellet Flame Temperature using Optical Pyrometry in Lab-scale Burner

지도교수 송 한 호

이 논문을 공학석사 학위논문으로 제출함

2014 년 2 월

서울대학교 대학원

기계항공공학부

송 정 우

송정우의 공학석사 학위논문을 인준함

2014 년 2 월

위 원 장 이 우 일 (인)

부위원장 송 한 호 (인)

위 원 김 민 수 (인)

Abstract

Measurement of Pulverized Wood Pellet Flame Temperature using Optical Pyrometry in Lab-scale Burner

Jeongwoo Song

Department of Mechanical & Aerospace Engineering

College of Engineering

Seoul National University

As increasing energy consumption, fossil fuels are on the brink of being exhausted and climate change occurs. Korea government adopts RPS (Renewable Energy Portfolio Standard) which deals with above problems in 2012. According to RPS programs, all the power corporation have to use renewable resources for 2 percent of total electric generation in 2012, and 10 percent of total power generation in 2022. Many power corporations adopt wood pellet power generation system because wood pellet is carbon neutral resource and weight factor of wood pellet is 2 in Korea RPS programs. However, fundamental research on wood pellet flame or combustion has not been performed sufficiently. In this study, we measured two dimensional temperature distribution of lab-scale pulverized wood pellet flame using two-color optical pyrometer. We calibrated optical system with tungsten filament lamp. To achieve the wood pellet flame in lab-scale burner, pulverized wood pellet particles were pre-heated and ignited by methane-air flat flame, where the particles were supplied by using a syringe pump and pneumatic vibrator. Finally, we could estimate two dimensional temperature field of the wood pellet flame by combining the calibration results and the signals from the flame.

Keywords: Wood pellet flame, Optical pyrometry, Flame temperature

Student Number: 2012-20674

List of Tables

List of Figures

Nomenclature

c	speed of light
$\bar{c}$	particle concentration
C	unit converge coefficient
d	particle diameter
E	extinction
h	planck constant
I	radiation intensity
k_B	boltzmann constant
K	absorption coefficient
KL	absorption strength
N	number of particles per unit volume
P	pixel value
S	spectral sensitivity
T	temperature
T_B	brightness temperature

Greek Letter

ϵ	emissivity
λ	wavelength
τ	optical depth

Subscripts

b,λ	blackbody spectral intensity
dL	infinitesimal length
red	red image
green	green image
λ	spectral intensity
0	initial beam intensity

1. Introduction

1.1. Research background

As increasing energy consumption, fossil fuels are on the brink of being exhausted and climate change occurs. In 2011, energy consumption in Korea to generate electricity accounts for 19 percent of total energy usage, and 64.8 percent of total fossil fuel usage.[1]

Korean government adopts RPS (Renewable Energy Portfolio Standard) to deal with the aforementioned issues in 2012. RPS is regulation that some portion of electricity generation should be derived from renewable resources. Since the RPS program takes effect, power corporations need to introduce new system using renewable energy sources for power generation.

According to RPS programs, each power corporations have to use renewable resources for 2 percent of total electric generation in 2012, and 10 percent of total power generation in 2022. The renewable fuels are categorized into solar energy and the others, for example IGCC(Integrated gasification combined cycle), waste matter, water power, bioenergy, RDF(Refuse Derived Fuel) and so on. Each energy source have weight factor defined by REC(Renewable Energy Certificate)renewable energy certificate(REC).

Among these resources, we focused on wood pellet. It has relatively high energy density (4500 kcal/kg) than other renewable resources. Wood pellet is widely used in combined heat and power plants in Northern Europe. Many power corporations adopt wood pellet power generation system because wood pellet is carbon neutral resource and weight factor of wood pellet is 2 in Korea RPS programs.[2] However, fundamental research on wood pellet flame or combustion has not been performed sufficiently. In this study, we focused on the temperature of the wood pellet flame, and measured two dimensional temperature distribution by using a lab-scale pulverized wood pellet burner and adopting two-color optical pyrometer.

1.2. Previous researches

There are many different method for measuring flame temperature, for example using thermocouple, gas sampling, optical pyrometer, CARS(Coherent Anti-stokes Raman Scattering) and using PLIF(Planar Laser Induced Fluorescence) imaging. Thermocouple is usually used to measure temperature[3,4], but there are some disadvantage using thermocouple. Flow field is interrupted by thermocouple, and thermocouple may be damaged by various particle inside solid fuel combustion. Especially, temperature measurement using thermocouple is point measurement, so measurement of temperature distribution in flow filed is difficult.

Temperature measurement method using CARS is accurate and non-intrusive diagnostics tool[5], but very expensive method and complicated. CARS system consists of high power laser, spectrometer and many optical devices, and optical devices have to be aligned very accurately. In addition, the CARS technique is also single-point temperature measurement.

There have been many studies on flame temperature measurement using optical pyrometer.[6,7] Optical pyrometer is a non-intrusive measurement method, having the possibility of measuring two-dimensional temperature distribution, and can be an inexpensive method, since a commercial digital camera can be used as a detector. However, optical pyrometer is highly affected by calibration data.

1.3. Research subjects

In this paper, we measured two dimensional temperature distribution of lab-scale pulverized wood pellet flame using two-color optical pyrometer. We used commercial digital camera, narrow band-pass filter, and beam-splitter. These imaging system was calibrated using tungsten filament lamp.

Lab-scale pulverized wood pellet flame was generated by center tube type Mckenna burner. From the two-color images of the pulverized wood pellet flame, we calculated temperature distribution. In calculating temperature distribution, we had to assumed emissivity of flame and for which Hottel and Broughton model was used.

2. Background

In this section, wood pellet combustion process and detailed theory of two-color optical pyrometer are discussed.

2.1. Wood pellet combustion

Wood pellet combustion is divided into two processes, one is solid-state combustion and the other is gas-state combustion. Wood pellet is composed of ash, tar, char, water and volatile matter. Combustion of the volatile matter occurs in gaseous phase, while the char oxidation is in solid phase.[8]

Wood pellet combustion processes include drying, volatilization, gas combustion and coke burnout. Gas state fuels are evaporated while volatilization process, then gas fuels are oxidized by environmental oxidizer. Diffusion flame is generated in gas-state combustion, so soot particle will be formed inside this region. Soot particles generated by volatile matter combustion is not significantly different from soot particles from gaseous fuel combustion.

Solid state combustion is maintained by char particle oxidization. Char combustion is simply described by carbon and oxygen reaction. 20% of the energy is released from char combustion. During char combustion, particle size is decreased, because carbon in char is converted to carbon dioxide and carbon monoxide. In typical solid-fuel combustion, time scale of the char combustion is around ten times longer than that of the volatile matter combustion.

2.2. Two-color pyrometer

Optical pyrometer is based on radiative heat transfer of heated particles. Especially two-color pyrometer uses the signals of two different wavelengths.

2.2.1. Radiative heat transfer

A particle with certain temperature transfers heat in radiation, convection, and conduction modes. We measure temperature of a particle by using radiative heat transfer. According to Planck's law, light intensity of black body with temperature T is given in Eqn. 2.1.

$$I_{\lambda,b} = \frac{2hc^2}{\lambda^5}\frac{1}{\exp(hc/\lambda k_B T) - 1} \qquad (2.1)$$

According to Eqn. 2.1, radiation intensity varies with body temperature and signal wavelength. If we measure radiation intensity at certain wavelength, we can estimate the temperature of the particle.

However, Eqn. 2.1 is only valid for the black body, and the realistic particles, e.g. soot, char, etc, are not black body. In this regard, emissivity of a particle is considered, which is the ratio of real particle's spectral radiance to spectral radiance of black body at the same temperature and wavelength. Eqn. 2.2 describes real particle radiation.

$$I_\lambda = \epsilon I_{\lambda,b} = \epsilon \frac{2hc^2}{\lambda^5} \frac{1}{\exp(hc/\lambda k_B T) - 1} \quad (2.2)$$

Optical pyrometer is based on radiative heat transfer of particles, so the particles must exist in the interested region of measurement. As mentioned in section 2.1, there are many particles in the domain of the pulverized wood pellet flame, where heated soot, char and ash emit radiations. This implies that the measured radiative signals from this region are the combined signals from soot, char and ash. Though these particles have the same temperature, spectral radiance intensity of each particle is different, which is related to the emissivity. The emissivity of these different particles are much dependent on the particle size, which will be discussed in details in the following section.

2.2.2. Emissivity model

Emissivity is related with absorption, extinction and scattering of a particle. Behavior of electromagnetic wave interacting with particle is described by Mie theory. Emissivity of particle is determined by particle size. According to Beer and Howarth, beam scattering with small particles like a soot is negligible, but scattering is not negligible for larger particles such as char and ash.[9]

It means that the emissivity of pulverized wood pellet flame can be very complicated, because there exist many particles such as soot, char, wood pellet particle and ash at the same time.

Since knowing the emissivity is essential for the temperature calculation in optical pyrometer, the use of proper emissivity model is important. There are many research using different emissivity model. Some researches assumed wavelength-dependent emissivity model for soot[7, 9], and adopted gray body assumption for char, solid fuel particle, and ash.[10, 11]

In this research, we adopted Hottel and Broughton emissivity model. In wood pellet flames soot is a dominant contributor for thermal radiation in flames, since the volatile matter in wood pellets accounts for about 80 % of the total mass and the soot is formed in the gas state combustion of these volatiles. The usage of the Hottle and Broughton model is also justified, because it has been used many times in the analysis of the pulverized coal flame where less soots are developed than wood pellet combustion. Following Hottel and Broughton emissivity model, we assume that the emissivity of pulverized wood pellet flame is wavelength dependent.

2.2.3. Two-color pyrometer

We measured radiation intensity with commercial digital cameras that have complementary-metal-oxide-semiconductor(CMOS) sensor. Each digital camera pixel has selective wavelength transmission. Generally, digital camera imaging sensor assumes Bayer pattern arrangement. A group of four pixels becomes the base unit of the Bayer pattern arrangement, i.e. two green pixels, one red pixel, and one blue pixel.

Each pixel detects a band of wavelengths, and color filter above optical detector has transmissivity along wavelengths. However, since the transmissivity of each color filter is not known to us from the manufacturer of the camera, we used the narrow band pass filters for narrow wavelength transmission. We measured radiation signals from pulverized wood pellet flames using two digital cameras and two narrow band pass filters. One camera detected red (623 - 643 nm) light signals, the other detected green (530 - 540 nm) lights.

To get pixel signals, we used digital raw files instead of compressed image files. DcrawMS program was used converting digital raw files to TIFF images. DcrawMS program has many options, where we used the options, such as (use the exact option names as shown in the program) “don’t use an embedded color matrix”, “raw output colorspace”, “don’t automatically brighten the image”, “linear 16-bit format”, and “document mode without scaling”. We used these options for getting the pure raw data. We received original pixel values by using the above options. Then we extracted separated RGB color images from raw images. Based on these processes, we measured red and green radiative signals using two digital cameras with narrow band pass filters.

Before measuring and calculating flame temperature distribution, we had to obtain calibration data relating pixel values with radiation signals. Calibration was conducted by using Philips tungsten filament lamp. Detailed calibration process and data will be written in section 3. Pulverized wood pellet flame images were interpreted by applying the calibration data.

Radiative beam intensity from infinitesimal thickness pulverized wood pellet flame can be described as in Eqn. 2.3.[12] Initial beam intensity is weaken by scattering and absorption. Scattering and absorption strength is determined by particle concentration, particle size, and extinction strength. I_{dL} is a infinitesimal thickness flame radiation intensity, I_0 is initial beam intensity, τ is optical thickness. $\bar{c}$ is particle concentration in unit volume, E is extinction strength, N is a number of particles, and d is diameter of particle.

$$I_{dL} = I_0 \exp(-\tau) = I_0 \exp[\bar{c}\ dL \sum_z E_{z\lambda} N_z (\pi d_z^2/4)] \quad (2.3)$$

To obtain total radiative intensity from flame, Eqn. 2.4 is integrated along the flame thickness.[13]

$$I_\lambda = \int_0^L I_{dL}\, dL = \int_0^L I_{\lambda,b} \exp(-\tau) dL = I_{\lambda,b}\, [1-\exp(-\tau_L)] \qquad (2.4)$$

According to above Eqn., emissivity of flame can be expressed as in Eqn. 2.5.

$$\epsilon_\lambda = 1-\exp(-\tau_L) = 1-\exp[-\bar{c} L K_\lambda] \quad (2.5)$$

K_λ is absorption coefficient. Small particles like a soot can neglect scattering, so emissivity is simply determined. Hottel and Brougton approximated extinction coefficient. Then emissivity can be described only by wavelength-dependent function in Eqn. 2.6.

$$\epsilon_\lambda \equiv 1 - \exp[-KL/\lambda^\alpha] \qquad (2.6)$$

KL is absorption strength that is independent of wavelength. and α is a constant over the visible wavelength.

Then, the pixel value measured by camera image sensor represents integrated flame radiation over the wavelength, area and exposure time. C is unit converging factor, T_λ is transmissivity of optical system, and S_λ is spectral response of imaging sensor.

$$P = C\int_{t_1}^{t_2}\int_{\lambda_1}^{\lambda_2}\int_A I_\lambda T_\lambda S_\lambda \, dA \, d\lambda \, dt \qquad (2.7)$$

We used narrow band pass filter, so Eqn. 2.7 can be simplified to Eqn. 2.8.

$$P = C(\lambda_2 - \lambda_1)\int_{t_1}^{t_2}\int_A I_\lambda T_\lambda S_\lambda \, dA \, dt \qquad (2.8)$$

To calculate temperature in Eqn. 2.8, the unknown variable KL should also be determined. Thus, we measured flame radiation intensity along two different wavelengths for two unknowns, i. e. temperature and KL.

2.3. Brightness temperature

Calibration data is given by a function of pixel value and brightness temperature not true temperature, because we used tungsten filament lamp for calibration instead of black body furnace. Tungsten is not a black body, so emissivity varies with temperature and wavelength. Tungsten filament radiation intensities were different than black body radiation at the same temperature. Thus, brightness temperature was used to compensate emissivity effects.

Emissivity of tungsten is well known, so we could convert temperature to brightness temperature. We used brightness temperature instead of true temperature, because flame emissivity was not known. Flame radiation intensity was affected by flame emissivity. In pulverized wood pellet flame, heated soot, char, and wood pellet particle emitted radiation signals. Calculating method of those particle emissivity was introduced in section 2.2.

Brightness temperature is the temperature of a black body having the same radiation intensity at a given wavelength as measured from the real particles. Brightness temperature is simply written as in Eqns. 2.9 and 2.10

$$I_{\lambda} = \epsilon_{\lambda} \frac{2hc^2}{\lambda^5} \frac{1}{\exp(\frac{hc}{k_B T \lambda}) - 1} = \frac{2hc^2}{\lambda^5} \frac{1}{\exp(\frac{hc}{k_B T_B \lambda}) - 1} \qquad (2.9)$$

$$T_B = \frac{hc}{k_b\lambda}\frac{1}{\ln(\frac{1}{\epsilon_\lambda}(\exp(\frac{hc}{k_B T\lambda})-1)+1)} \qquad (2.10)$$

Brightness temperature is not affected emissivity of object, so we could measure brightness temperature of the flame using calibration data that has the relationship between brightness temperature of tungsten filament and pixel values. Then we calculated flame emission by using flame emissivity model, and we could convert brightness temperature to real flame temperature using Eqn. 2.11.

$$T = \frac{hc}{k_b\lambda}\frac{1}{\ln(\epsilon_\lambda(\exp(\frac{hc}{k_B T_B\lambda})-1)+1)} \qquad (2.11)$$

3. Calibration

Calibration procedure is important, because flame images were directly convert to brightness temperature using calibration data. Calibration results determined wood pellet flame temperature. Thus, detailed calibration devices set-up and results are discussed, in this section.

3.1. Calibration set-up

Detecting parts consisted of two commercial digital camera(Nikon D5200), two narrow band pass filter(Andover 550FS10-50, Andover 633FS10-50), two camera lens(Nikon 50mm F1.4) and one beam splitter(Edmund optics standard plate beamsplitter 50R/50T). Camera setting was ISO 1000, F = 4.0 and 1/1000 seconds exposure time. This detecting set-up is the same as the one in pulverized wood pellet flame experiments. In figure 3.1, calibration devices configuration is shown.

Tungsten filament lamp used in calibration procedure was Philips W21W lamp. Electric currents was controlled by DC power supply(Protek PL 3003s). Current range was from 0.568 A to 1.03 A. Lamp was located center tube of Mckenna burner, because solid angle of radiation was maintained the same between tungsten filament and pulverized wood pellet flame. Pixel value of imaging sensor was affected particle temperature, emissivity, detecting wavelength range, exposure time, transmissivity, spectral response, and solid angle. Solid angle was related to collecting angle of each pixels, so collecting angle should be the same both in calibration and experiment. For this reason, we kept tungsten filament lamp at the same location as the region of interest in pulverized wood pellet flame experiments.

There was a study that calculates tungsten filament temperature.[14] They measured filament temperature while varying electric current. Metals like a tungsten have different resistance along the temperature. Generally, resistance of metals increases with temperature. Therefore, resistance of tungsten filament indicates temperature of tungsten. Resistance is a function of specimen area, length, and specific resistance. Those properties are changing with temperature, but mechanical and electrical properties tungsten are well known. Thus, we could find a tungsten property table relating the tungsten filament resistance and the temperature.[15] Our measurement showed similar results, as compared to the reference data. Finally, we captured lamp images with temperature range from 1000 K to 1400 K. In figure 3.2, a relation of electric currents and tungsten filament temperature is shown.

As mentioned earlier, camera images were loaded in MATLAB using dcrawMS programs. The loaded raw image files were in a 14-bit format. Then, we divided these raw image data into red, green, and blue ones. Out of these color data, only the tungsten filament region was extracted and the pixel values were averaged. Five images were taken for each temperature, and we used the mean value of these five lamp images. Temperature was converted to brightness temperature by considering spectral emissivity of tungsten in visible wavelength range. Finally, we could achieve a function of pixel value and brightness temperature.

Here, it is noted that tungsten spectral emissivity was already measured by many researchers in various temperatures and wavelength ranges. Our calibration was conducted with temperature range 1000 K to 1400 K, so we had to use an appropriate set of measured tungsten filament emissivity.

3.2. Calibration results

Figures 3.3 and 3.4 show lamp images with varying currents. We can convert these currents to certain temperatures by using the property table, or as shown in Figure 3.2. Saturation level of image sensor was 16384, so we controlled the current to prevent lamp image intensity from exceeding the saturation level.

By following the procedures in section 3.1, a function of brightness temperature and pixel value is fitting by using Eqn. 3.1. We calculated two curves for red and green, which covert each pixel value to brightness temperature.

$$P_{red} = a_r \times {T_{B,red}}^{b_r} + c_r, P_{green} = a_g \times {T_{B,red}}^{b_g} + c_g \qquad (3.1)$$

The fitting coefficients are listed in table 3.1

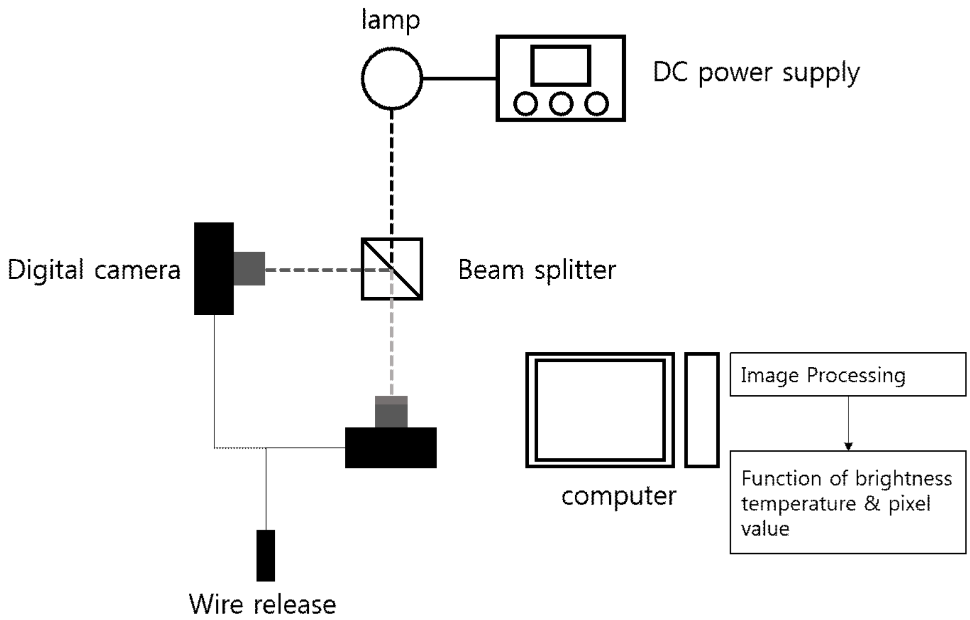

Figure 3.1 Calibration devices configuration

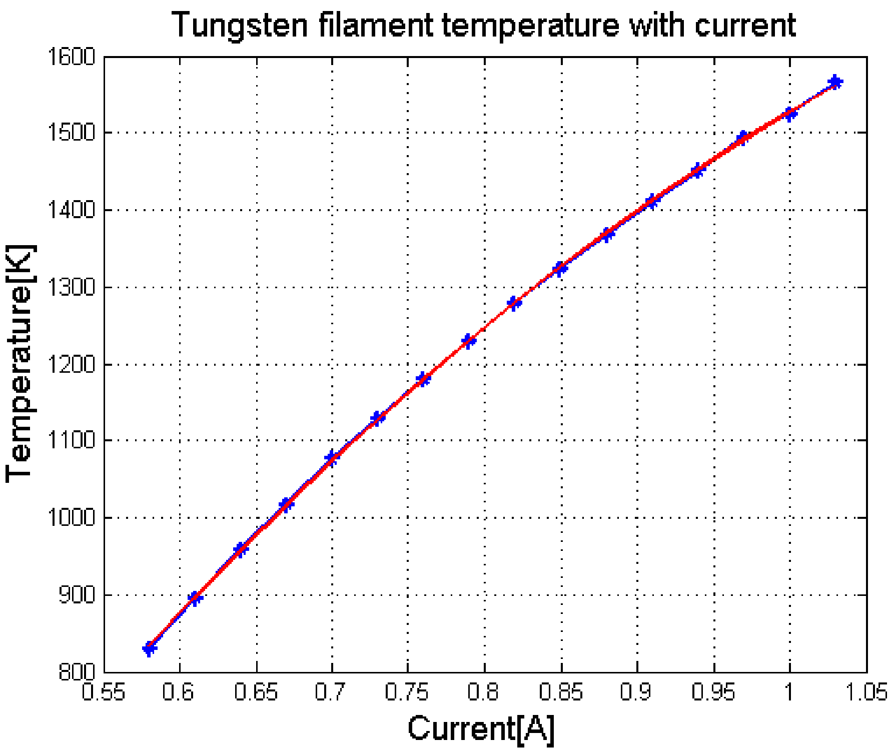

Figure 3.2 Tungsten filament temperature variation with currents change

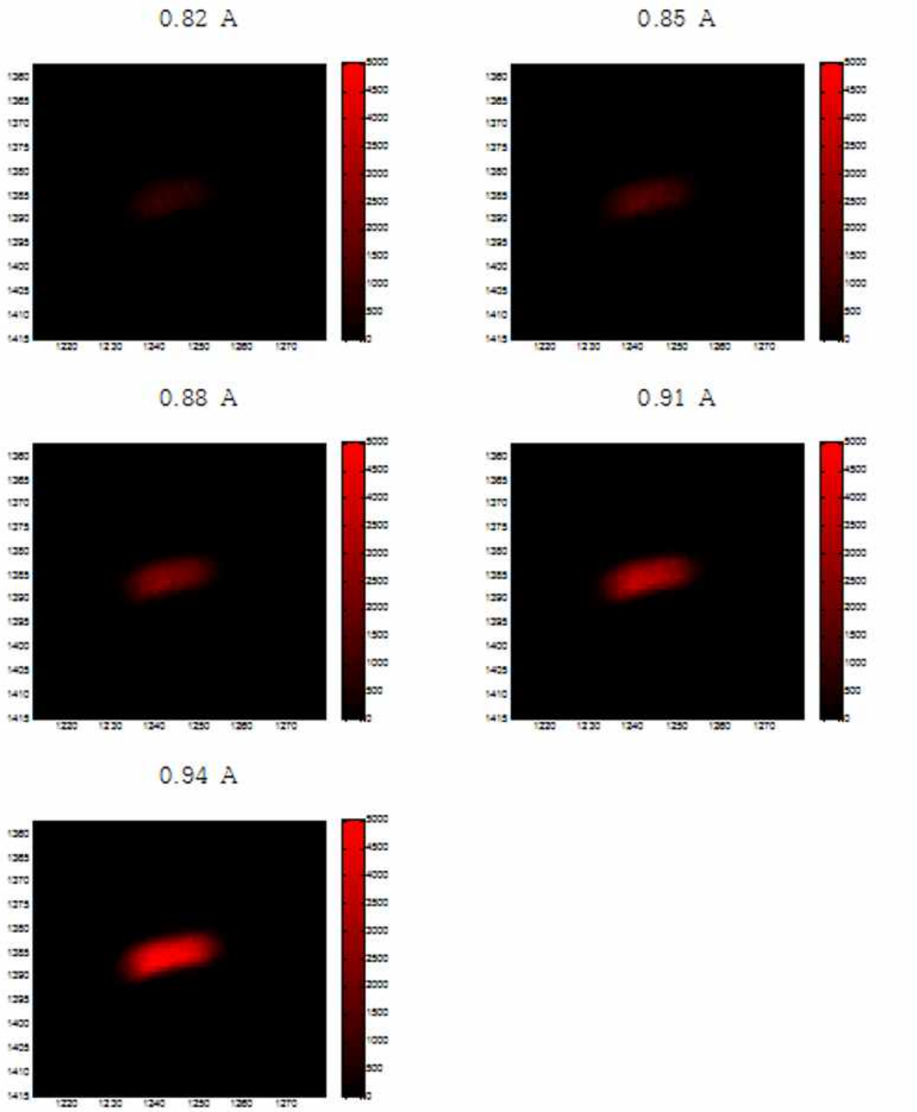

Figure 3.3 Red(633 nm) band pass filtered tungsten filament images with various currents

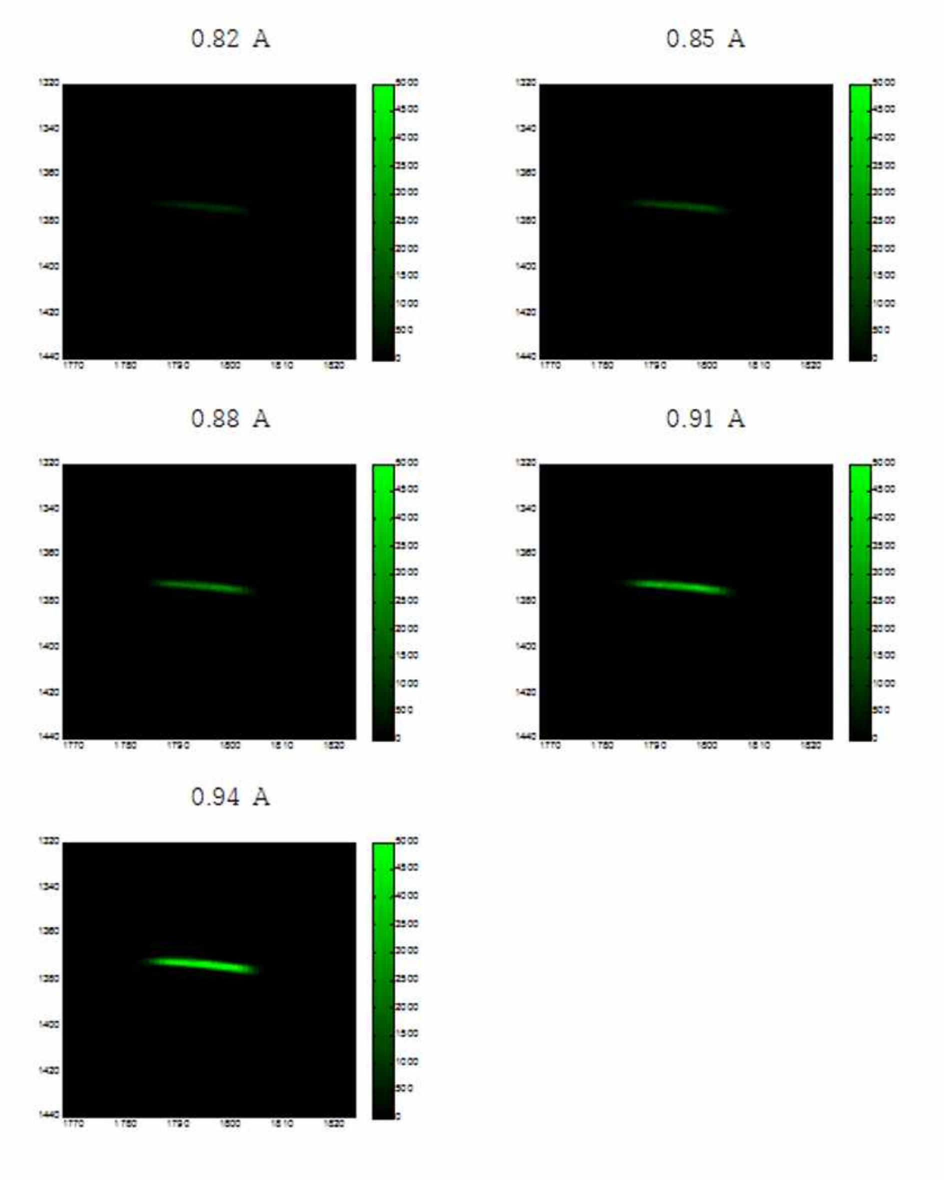

Figure 3.4 Green(550 nm) band pass filtered tungsten filament images with various currents

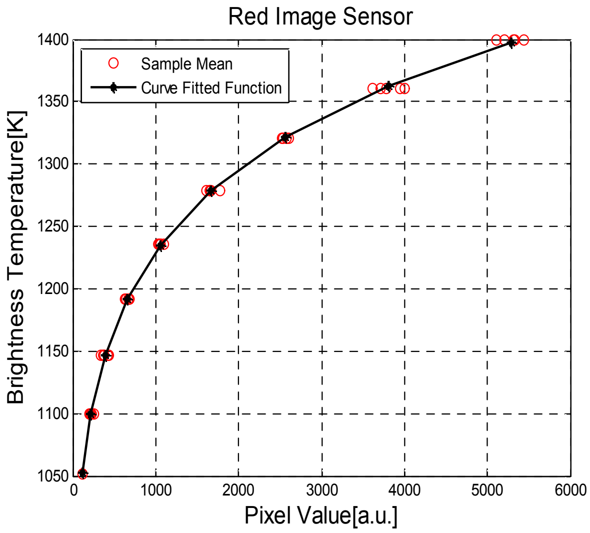

(a)

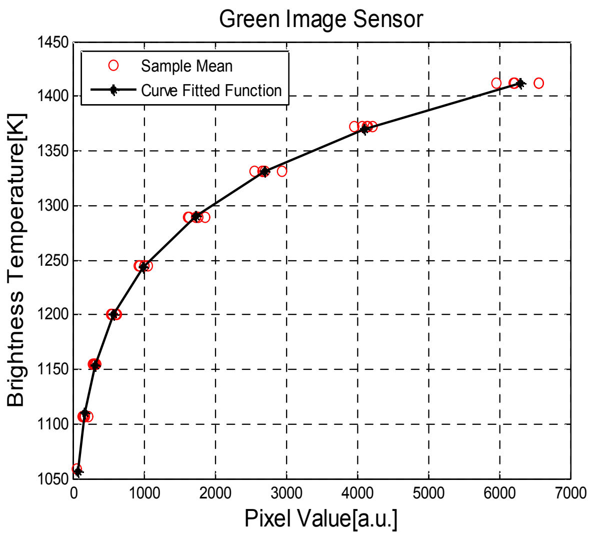

(b)

Figure 3.5 Relation between brightness temperature and pixel value: (a) Red, (b) Green

Table 3.1 Coefficients of curve fitted function that correlates pixel value and brightness temperature

a_r	b_r	c_r
438.9	0.1033	333.8
a_g	b_g	c_g
330.0	0.1137	520.3

4. Experiments

In this section, experimental set-up and experimental devices are explained. Experimental parts consisted of burner, particle feeder, and detecting system. Detailed descriptions for individual devices will be discussed section 4.2.

4.1. Experimental set-up

Overall experimental set-up is shown in Figure 4.1. Experimental set-up is similar to the calibration set-up. As mentioned earlier, detecting part of the set-up is the same as the one in calibration, which has two commercial digital cameras, two narrow band pass filter, and one beam splitter. All the detecting devices adopted the exactly same conditions as in the calibration procedures, because image sensor signals were affected not only by particle temperature but also by detecting system conditions, such as exposure time, sensitivity, f number, focal length and wavelength range. For example, image sensor signal linearly increases with exposure time, increasing sensitivity, and decreasing f number. Focal length affects resolution of images and wavelength range of band pass filter also affects sensor signal.

Pulverized wood pellet flame was produced by center-tube-type Mckenna burner. Detailed burner description will be discussed in section 4.2. In the burner, pulverized wood pellet particles, carried by air, were heated and ignited by methane-air flat flame. The particle feeder design will also be discussed in section 4.2. Methane, air, and carrier gas flow rates were controlled by mass flow controller(MKS, 1179A53CS18V)

4.2. Experimental devices

Pulverized wood pellet flame was produced by center-tube-type Mckenna burner. The wood pellet particles were fed into the burner by an in-house particle feeder. In this section, detailed burner and particle feeder design will be discussed.

4.2.1. Pulverized wood pellet burner

Center-tube-type Mckenna burner consisted of sintered stainless burner plug, shroud ring, and center tube. Methane and air flew across the sintered stainless burner plug. Blue premixed methane and air flat flame was slightly detached on water cooled sintered stainless burner plug. Methane-air premixed flame was used to heat wood pellet particles. For the methane inlet pipe, we installed a flame arrestor that prevents flash back. Two static mixers are used to premix the methane and air, so premixed mixture can be supplied to Mckenna burner.

Particles were entered into the flat flame zone through the center tube of the burner. Particles were heated by methane-air flat flame, then water and volatile matters were evaporated. Volatile matters were ignited by surrounding heat that was produced by flat flame. In this way, gas state combustion of pulverized wood pellet flame was induced, which also led to char oxidation process in the downstream.

4.2.2. Particle feeding system

Particle feeder consisted of syringe pump, pneumatic vibrator, and carrier gas lines. Firstly, particles were partially filled in the syringe, which was installed in a syringe pump. Syringe pump was used to keep the surface level of wood pellet particle in the syringe, as the particles were blown out and fed to the burner. Maintaining the particle level was essential, because particle feeding rates were determined by carrier gas flow rate and blown particle density inside the syringe and the particle feeding line. For example, in the same carrier gas flow rate, particle feeding rates were low at low blown particle density inside the syringe and the particle feeding tube. If we actuate syringe pump to raise the piston to increase blown particle density inside the syringe, particle feeding rates were increased and then converged.

We modified syringe to carry particles. Piston side of syringe was maintained, but the injection side was cut out. We made a cylindrical part that fit the syringe and had two holes. One hole was inlet of carrier gas, and the other was the outlet of the aerosol form of particles and carrier gas mixture. The cylindrical part and the syringe body was sealed by using the rubber ring of the original piston.

Pneumatic vibrator was used to prevent deposition or adhesion of particles. Particles were deposited on the inner surface of the syringe or the feeding line, so there needed some vibration to float particles. Pneumatic vibrator installed on syringe, so its vibration force was transferred to syringe and particle feeding tube. By this vibrating motion, particle feeding could be smooth and continuous.

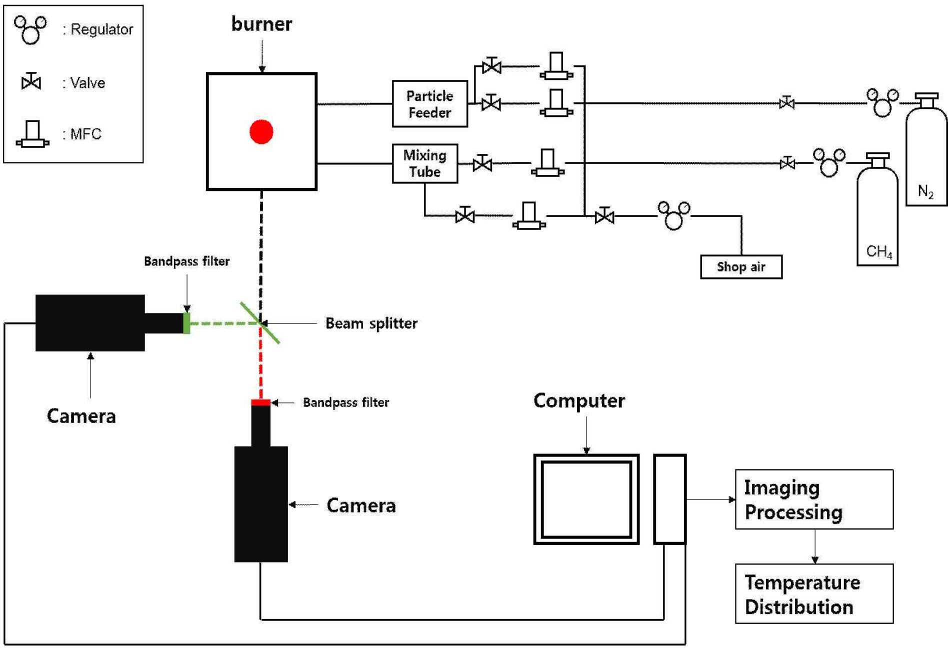

Figure 4.1 Experimental devices configuration

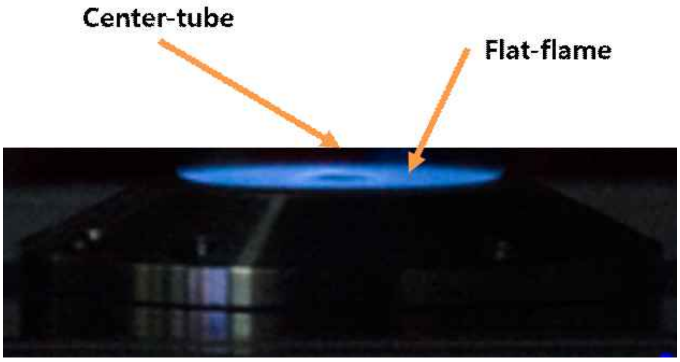

(a)

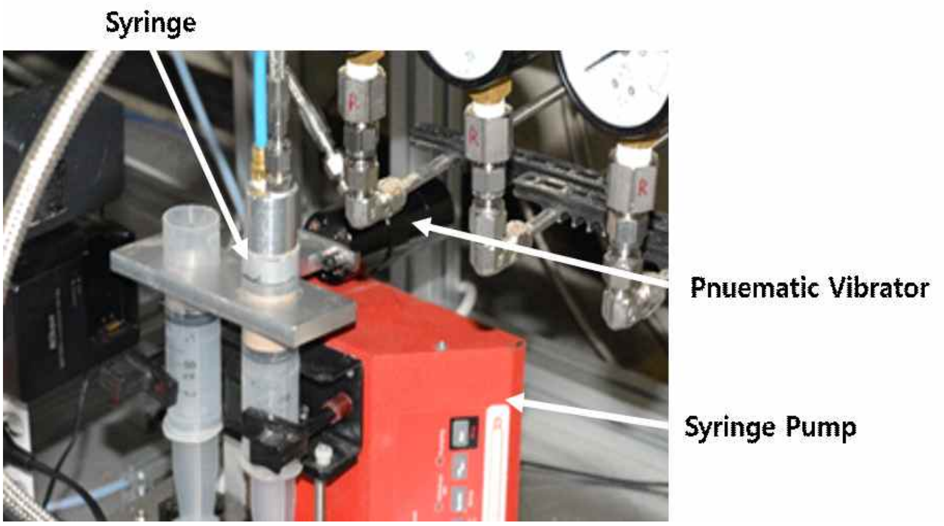

(a)

Figure 4.2 Experimental devices image: (a) Flat flame burner configuration, (b) particle feeding system

5. Experimental results

Experiment condition is listed in Table 5.1. Pulverized wood pellet particles carried by air were ignited by surrounding heat from methane-air flat flame. At low flow rate of carrier gas, particle behavior was observed. At high flow rate of carrier gas and high density of particles, however, diffusion jet flame similar to the one of gaseous fuel was formed.

The chosen experimental condition was for the high flow rate of carrier gas and high particle density inside the syringe, and thus we could achieve luminous flame images. At high flow rates of pulverized wood pellet particles, wood pellet flame looks like a diffusion flame. At low flow rates, we distinguished wood pellet particles in flame. Thus, we assumed that emissivity model was Hottel and Broughton model that usually well describe soot emissivity.

In figure 5.1, there are shown pulverized wood pellet flame image and narrow band pass filtered images. Pulverized wood pellet was heated by methane-air flat flame. Wood pellet particles were ignited, and pulverized wood pellet flame was formed. As mentioned earlier, red and green flame images were taken using two digital cameras with narrow band pass filter. Then, we converted pixel value to brightness temperature using calibration data. Finally, we calculated true temperature of flame and true temperature distribution is shown in Figure 5.2. Two dimensional temperature distribution was measured using two-color optical pyrometry. Average temperature of wood pellet flame was 1445 K. Combustion gas was lean, so wood pellet flame temperature at nearly stoichiometric combustion may be higher than this experiment results.

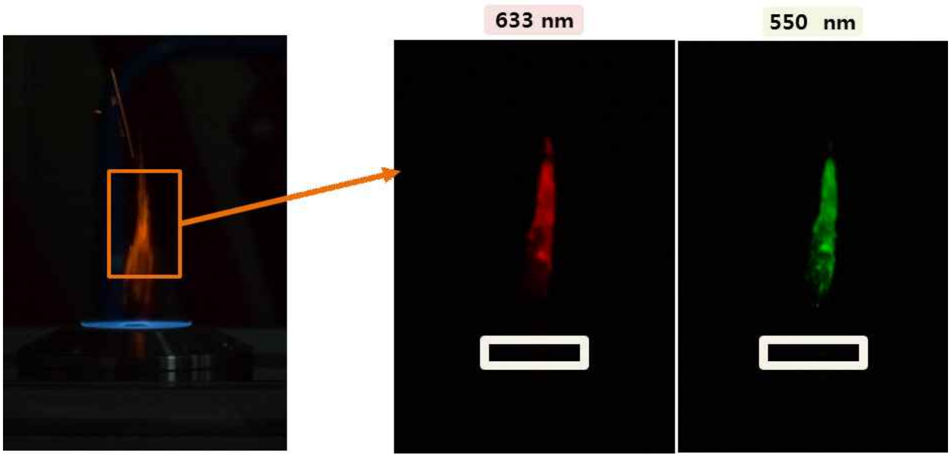

Figure 5.1 Pulverized wood pellet flame image and narrow band pass filtered flame images

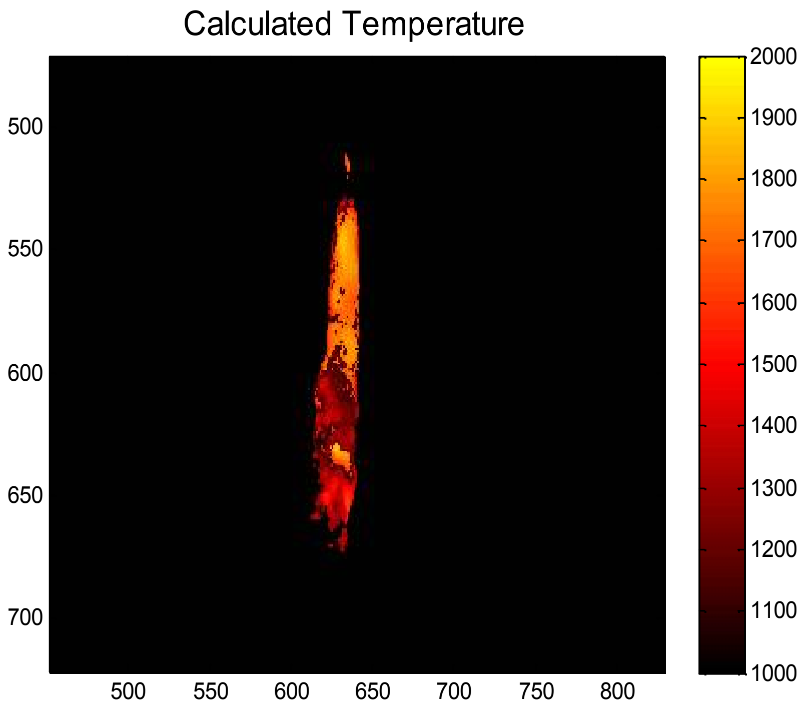

Figure 5.2 Pulverized wood pellet flame temperature distribution

Table 5.1 Experimental condition

Flat flame air flow rates	16500 sccm
Flat flame methane flow rates	1300 sccm
Equivalence ratio	0.75
Carrier gas(air) flow rates	2265 sccm
Syringe pump pumping rates	5.1 ml/min
Cooling water flow rates	0.5 L/min

6. Conclusion

In this study, we measured two dimensional temperature distribution of the pulverized wood pellet flame by using two-color optical pyrometry. Calibration of optical system was conducted with tungsten filament lamp and DC power supply. We used raw image files of color digital cameras, from which a calibration function between image sensor signals and brightness temperature was obtained. Detection set-up was rather simple where we could use commercial digital cameras. Thus, the developed method can be adapted to the industrial scale burner without significant changes. In this research, we experimented in lab-scale pulverized wood pellet flame. We used Mckenna burner for making lab-scale wood pellet flame. In a center-tube-type Mckenna burner, we could produce methane-air flat flame stabilized pulverized wood pellet flame, and we measured red and green brightness temperature of the flame using tungsten filament calibrated optical system. Measured images were processed by MATLAB image processing toolbox. were processed by MATLAB image processing toolbox. Firstly, we determined the amount of image shifts from two camera images by using cross correlation method. Then, we calculated the flame temperature using calibration data. Here, an appropriate emissivity model was used to convert brightness temperature to the true temperature of flames, where we adopted Hottel and Broughton emissivity model for soot particles.

Here is the summary of the findings:

1. Red and green brightness temperature are measured from 1000 to 1400 K using our detection system and calibration settings. To measure higher or lower temperature region has to change digital camera settings and calibration lamp currents.
2. We used Hottel and Broughton emissivity model to estimate true temperature of the flame from the brightness temperature. Although radiation signal sources in pulverized wood pellet flame are not only soot but also char, ash and wood pellet particles, we assumed that the dominant radiation source from the wood pellet flame was soot. Based on these approximations, true temperature of flame in our experimental condition ranged from 1100 to 1800 K.

References

1. 2012, Yearbook of Energy Statistics 2012, Ministry of Knowledge Economy
2. 2013, RPS oprating instructions, Ministry of Knowledge Economy
3. Tdaaaki Shimizu, Jun Han, Sunyoung Choi, Leahyun Kim, Heejoon Kim, 2006, Fluidized-Bed combustion characteristics of cedar pellets by using an alternative bed material, Energy & Fuels, 20, pp. 2737-2742
4. Sonnik Clausen, 1996, Local measurement of gas temperature with an infrared fiber-optic probe, Meas. Sci. Technol., 7, pp. 888-896
5. M. Pealat, P. Bouchardy, M. Lefebvre, J.-P. Taran, 1985, Precision of multiplex CARS temperature measurements, Applied Optics, 24, pp. 1012-1022
6. Gang Lu, Yong Yan, Steve Cornwell, Michael Whitehouse, Gerry Riley, 2008, Impact of co-firing coal and biomass on flame characteristics and stability, Fuel, 87, pp. 1133-1140
7. Gang Lu, Yong Yan, 2006, Temperature profiling of pulverized coal flames using multicolor pyrometric and digital imaging techniques, IEEE, 55, pp. 1303-1308
8. Colomba Di Blasi, 1993, Modeling and simulation of combustion processes of charring and non-charring solid fuels, Prog. Energy Combust. Sci., 19, pp. 71-104

9. Gang Lu, Yong Yan, Gerry Riley, Harrish Chandr Bhemmul, 2002, Concurrent measurement of temperature and soot concentration of pulverized coal flames, IEEE transactions on instrumentation and measurement, vol. 51, no. 5, pp. 990-995
10. David W. Shaw, Robert H. Essenhigh, 1991, Temperature fluctuations in pulverized coal(P.C.) flames, Combustion and flame, 8, pp. 333-346
11. Zixue Luo, Huai-Chun Zhou, 2007, A combustion-monitoring system with 3-D temperature reconstruction based on flame-image processing technique, vol. 56, no. 5, pp.1877-1882
12. J. M. Beer, C. R. Howarth, 1969, Radiation from flames in furnaces, Symposium (International) on Combustion, vol. 12, issue 1, pp. 1205-1217
13. Teri Snow Draper, 2012, Application of two-color pyrometry to characterize the two-dimensional temperature and emissivity of pulverized-coal oxy-flames, Brigham Young University
14. Charles de Izarra, Jean-Michel Gitton, 2010, Calibration and temperature profile of a tungsten filament lamp, European Journal of Physics, 31, pp. 933-942
15. P.D Desai, T.K. Chu, H.M James, C. Y. Ho, 1984, Electrical resistivity of selected elements, J. Phys. Chem. Ref. Data, vol. 13, No.4, pp. 1069-1096

요약

광학고온계측법을 이용한 미분 우드펠릿 화염의 온도 측정

서울대학교 대학원
기계항공공학부
송정우

환경오염에 따른 문제 때문에, 한국에서는 2012년부터 RPS제도를 도입하였다. 이에 따라, 발전사들은 기존의 화석연료 외에 다른 신재생에너지원을 이용하여 일정부분 발전을 해야만 하는 상황이다. 여러 신재생에너지원 중 기존 화력발전소에서 이용할 수 있으며, RPS제도의 가중치가 높은 우드펠릿에 주목하였다. 우드펠릿을 이용한 발전의 수요는 늘어가지만, 우드펠릿 화염에 관한 기초연구는 부족하였다. 따라서 화염의 여러 가지 인자 중 온도측정을 목표로 하여 연구를 진행하였다. 화염 부분은 온도가 상당히 높기 때문에, 온도측정방법이 제한적이고, 화염 유동 장에 방해를 주지 않으며 온도를 계측하기 위하여 광학고온계측법을 도입하여 실험을 수행하였다. 광학고온계측법은 실험 셋팅이 레이저를 이용한 온도측정에 비하여 단순하고, 2차원 온도 분포를 측정할 수 있다는 장점이 있다. 이번 연구에서는, 디지털 카메라를 이용하여 실험을 수행하였으며, 텅스텐램프를 이용하여 온도에 대한 교정을 수행하였다. 평면화염버너를 이용하여 미분화된 우드펠릿에 열을 가하여, 우드

펠릿 화염을 안정화 시켰다. 미분화된 우드펠릿은 시린지 펌프와 공압 바이브레이터를 이용하여, 평면화염버너의 중심 관으로 공급하였다. 이와 같은 구성을 통하여 미분화된 우드펠릿 화염을 실험실 환경에서 모사할 수 있었으며, 텅스텐램프를 이용한 교정결과를 적용하여 화염의 2차원 온도분포를 구할 수 있었다.

주요어: 우드펠릿 화염, 광학고온계측법, 화염 온도
학번: 2012-20674